



Emerging investigator series: Primary emissions, ozone reactivity, and byproduct emissions from building insulation materials

Journal:	<i>Environmental Science: Processes & Impacts</i>
Manuscript ID	EM-ART-01-2019-000024.R1
Article Type:	Paper
Date Submitted by the Author:	06-Mar-2019
Complete List of Authors:	Chin, Kyle; Portland State University, Mechanical and Materials Engineering Laguerre, Aurelie; Portland State University, Mechanical and Materials Engineering Ramasubramanian, Pradeep; Portland State University, Mechanical and Materials Engineering Pleshakov, David; Portland State University, Mechanical and Materials Engineering Stephens, Brent; Illinois Institute of Technology, Civil, Architectural, & Environmental Engineering Gall, Elliott; Portland State University, Mechanical and Materials Engineering

Environmental Significance Statement:

Building enclosures affect indoor air through primary pollutant emissions from building materials, filtering outdoor air, and secondary emissions from reactions between oxidants (such as ozone, O₃) and materials within cavities. Infiltration of outdoor air across the building envelope is often the dominant pathway by which ambient O₃ (a primary driver of oxidation chemistry in buildings) penetrates indoors, particularly in residences. This work investigates primary VOC emissions, O₃ reaction probabilities, and O₃ reaction byproduct formation yields from eight insulation materials commonly used in building enclosures. To our knowledge, this study provides the broadest characterization of these properties for building insulation materials to date. Parameterizations reported here can enable models of outdoor-to-indoor O₃ transport and inform material selection to reduce an overlooked source (wall cavity materials) of VOCs to the indoor environment.

Emerging investigator series: Primary emissions, ozone reactivity, and byproduct emissions from building insulation materials

Kyle Chin¹, Aurelie Laguerre¹, Pradeep Ramasubramanian¹, David Pleshakov¹, Brent Stephens², Elliott T. Gall^{1,*}

¹ Portland State University, Mechanical and Materials Engineering, Portland, OR USA

² Illinois Institute of Technology, Civil, Architectural, and Environmental Engineering, Chicago, IL USA

*Corresponding email: gall@pdx.edu

ABSTRACT

Building insulation materials can affect indoor air by (i) releasing primary volatile organic compounds (VOCs) from building enclosure cavities to the interior space, (ii) mitigating exposure to outdoor pollutants through reactive deposition (of oxidants, e.g., ozone) or filtration (of particles) in infiltration air, and (iii) generating secondary VOCs and other gas-phase byproducts resulting from oxidant reactions. This study reports primary VOC emission fluxes, ozone (O₃) reaction probabilities (γ), and O₃ reaction byproduct yields for eight common, commercially available insulation materials. Fluxes of primary VOCs from the materials, measured in a continuous flow reactor using proton transfer reaction – time of flight – mass spectrometry, ranged from 3 (polystyrene with thermal backing) to 61 (cellulose) $\mu\text{moles}/\text{m}^2/\text{h}$ (with total VOC mass emission rates estimated to be between ~ 0.3 and ~ 3.3 $\text{mg}/\text{m}^2/\text{h}$). Major primary VOC fluxes from cellulose were tentatively identified as compounds likely associated with cellulose chemical and thermal decomposition products. Ozone-material γ ranged from $\sim 1 \times 10^{-6}$ to $\sim 30 \times 10^{-6}$. Polystyrene with thermal backing and polyisocyanurate had the lowest γ , while cellulose and fiberglass had the highest. In the presence of O₃, total observed volatile byproduct yields ranged from 0.25 (polystyrene) to 0.85 (recycled denim) moles of VOCs produced per mole of O₃ consumed, or equivalent to secondary fluxes that range from 0.71 (polystyrene) to 10 (recycled denim) $\mu\text{moles}/\text{m}^2/\text{h}$. Major emitted products in the presence of O₃ were generally different from primary emissions and were characterized by yields of aldehydes and acetone. This work provides new data that can be used to evaluate and eventually model the impact of “hidden” materials (i.e., those present inside wall cavities) on indoor air quality. The data may also guide building enclosure material selection, especially for buildings in areas of high outdoor O₃.

KEYWORDS

Ozone reaction probability; PTR-TOF-MS; Volatile organic compounds; Reaction byproducts; Yields

1 INTRODUCTION

Building envelopes impact indoor air quality in three general ways: (i) primary emissions of air pollutants from materials used in the enclosure to the interior space, (ii) incidental removal of outdoor air pollutants that cross the enclosure through reactive deposition of oxidants (such as ozone, or O₃) or filtration of particles, and (iii) secondary emissions of air pollutants resulting from reactions between infiltrating oxidants (e.g., O₃) and materials used in the enclosure. Whether the impact of the building enclosure on indoor air quality is beneficial or detrimental to the exposure of occupants is dependent on a large number of factors, including (but not limited to) material selection, environmental conditions, airflow characteristics, and the quantity and type of indoor and outdoor air pollutants present.

Through emission, removal, and transformation, building enclosures impact the balance of indoor volatile organic compounds (VOCs) and O₃. Volatile organic compounds are a well-studied class of indoor air pollution, and VOCs often exceed chronic health standards indoors.¹ Ozone is a major driver of indoor chemistry and one of the most studied oxidants in indoor air.² Elevated concentrations of outdoor, ground-level O₃ are consistently associated with increases in a number of adverse health effects including mortality,³⁻⁵ exacerbation of asthma symptoms,⁶ and infant respiratory and cardiovascular effects.⁷ In 2005, ambient O₃ was estimated to account for ~4,700 deaths and ~36,000 years of life lost in the United States alone, suggesting that despite significant improvements in outdoor air quality in recent decades, levels of outdoor O₃ still pose a risk to public health.⁸

Primary emissions of VOCs from materials in building enclosure cavities contribute substantially and directly to indoor VOC concentrations.⁹⁻¹¹ Building enclosure materials also act as a “hidden” transformation pathway as infiltration air enters a building. For example, in

1
2
3 the vast majority of residences in the U.S., which typically do not have mechanical ventilation
4 systems with dedicated outdoor air supply,¹² occupants are exposed to O₃ and O₃ reaction
5 byproducts (including VOCs) only after O₃-laden air penetrates through leaks in the building
6 enclosure.^{13–15} In U.S. residences, limited data suggests that windows are seldom open in most
7 climates, less than 15% of the time in most cases.^{16,17} Therefore, infiltration across the building
8 envelope is often the primary path by which O₃ and O₃-building enclosure reaction byproducts
9 enter occupied residential spaces.¹⁸ Cracks and gaps in the building enclosure where infiltration
10 occurs create the potential for O₃ chemistry with interior enclosure materials, such as exterior
11 cladding, insulation, and structural materials, depending on the reactivity of the materials used
12 and the nature of crack geometries.^{15,19,20} Reactions within the building enclosure can serve to
13 reduce the amount of outdoor O₃ that transports indoors through surface chemistry that alters
14 the balance of O₃ and may generate harmful or irritating O₃ reaction byproducts found indoors.
15
16
17
18
19
20
21
22
23
24
25
26
27
28
29
30
31
32

33 To date, O₃ penetration factors have been measured in only a very limited number of buildings.
34 In a sample of eight homes in Austin, TX, the first measurements of O₃ penetration factors
35 (measured at an artificially high indoor/outdoor pressure difference) ranged from as low as ~0.6
36 to as high as ~1.0.²¹ Subsequent measurements of O₃ penetration factors in a multi-family
37 apartment unit during natural infiltration conditions revealed a mean value of only 0.54.²² These
38 data suggest that most homes relying on infiltration for ventilation air likely have O₃ penetration
39 factors lower than unity (i.e., $P_{O_3} \leq 1$). In homes under these conditions, as much as 40-50% of
40 total outdoor O₃ loss occurred because of reactions within the building enclosure, offering
41 substantial protection from indoor ozone exposure, but with implications for subsequent
42 exposure to byproducts of O₃ reactions within the building enclosure that may be transported
43 indoors.
44
45
46
47
48
49
50
51
52
53
54
55
56
57
58
59
60

1
2
3 If O₃ reactions occur primarily at the enclosure, indoor exposures to infiltrated O₃ are likely
4
5 lower than if reaction losses occur primarily with indoor materials and reactive gas-phase
6
7 compounds. Indoor exposure to O₃ reaction byproducts formed from homogeneous or
8
9 heterogeneous indoor O₃ chemistry are also likely to be different, due to the distinct materials
10
11 that are present in building enclosures versus in interior occupied spaces. Some known
12
13 byproducts of indoor O₃ reactions with common surfaces and/or gases in typical indoor
14
15 environments include organic acids, carbonyls, free radicals, and secondary organic aerosols,²³⁻
16
17 ²⁶ all of which can yield varied inflammatory responses in humans. Understanding routes of
18
19 indoor O₃ removal and transformation are warranted given that O₃ oxidation products may be
20
21 partially responsible for the health impacts of ambient O₃ observed in epidemiology studies.¹⁶
22
23
24
25
26
27

28 Ozone reaction probabilities of typical building enclosure materials available in the literature
29
30 range several orders of magnitude, from ~10⁻⁴ for brick to ~10⁻⁸ for aluminum.¹⁵ Key material
31
32 properties that influence O₃ reaction probability are porosity, thickness, and composition.²⁷
33
34 However, there exists very limited data in the literature reporting O₃ reaction probabilities to
35
36 materials used inside building enclosures (e.g., various insulation types, soundproofing, etc.)
37
38 and little data reporting the emissions of volatile byproducts stemming from these materials in
39
40 the presence or absence of O₃. Therefore, this study evaluates primary VOC emissions, O₃
41
42 reaction probabilities, and O₃ reaction byproduct yields for eight common, commercially
43
44 available building insulation materials to further understanding of how insulation selection in
45
46 building enclosures may affect indoor air through these mechanisms.
47
48
49
50
51
52

53 **2 METHODS**

54 *2.1 Test materials*

55
56
57
58
59
60

1
2
3 Eight commercially available insulation materials that are commonly used in building
4 enclosures were selected to span a wide range of chemical composition and physical properties:
5 fiberglass, cellulose, stone wool, recycled denim, polystyrene, polyurethane spray foam,
6 polystyrene with a thermal backing, and polyisocyanurate foam. An overview of properties of
7 the test materials is provided in Table 1. Images of each tested material in its raw form and as
8 prepared for testing are provided in the Table S1 in the supporting information.
9
10
11
12
13
14
15
16
17
18

19 All tested materials were purchased new. A sub-sample of each material was randomly taken
20 from the larger quantity of each purchased product. Samples were made to accommodate
21 placement in a benchtop scale environmental chamber (see Section 2.2) for measurement of
22 VOC emissions, O₃ dry deposition, and reaction byproducts emitted after being exposed to O₃.
23 Materials were of varying morphology and bulk structure and were prepared to ensure a known,
24 projected surface area was exposed to the bulk chamber air. Materials made of loose fill
25 (cellulose, fiberglass, stone wool, denim) were placed in a glass enclosure (Pyrex) with taped
26 edges. Solid materials were cut with the sides and backing sealed with aluminium tape to expose
27 only the top surface to the chamber environment.
28
29
30
31
32
33
34
35
36
37
38
39
40
41
42
43
44
45
46
47
48
49
50
51
52
53
54
55
56
57
58
59
60

Table 1. Summary of characteristics of tested building enclosure materials

Manufacturer	Name/material ¹	Code	Sample mass (g)	Exposed area (cm ²)	v_t used ²
Owens Corning	Fiberglass	FG	11.8	74.6	FG
GreenFiber	Cellulose	C	54.9	74.6	C
Touch 'n Foam	Polyurethane	PU	31.3	88.1	PI
Thermasheath	Polyisocyanurate	PI	24.9	148.5	PI
Roxul	Stone Wool	SW	24.9	74.6	FG
R-Tech	Polystyrene w/ thermal backing	PSTB	11.8	136.2	PS
Cellofoam	Polystyrene	PS	8.1	145.9	PS
UltraTouch	Recycled denim	DM	25.3	74.6	FG

¹ An image of each material in its raw form and as prepared for testing is available in the supporting information

² FG = fiberglass, C = Cellulose, PI = Polyisocyanurate, PS = Polystyrene

2.2 Chamber apparatus and instrumentation

Samples were tested for source and sink behaviour in a 11.4 L laboratory chamber apparatus; detailed descriptions of a similar experimental apparatus are available in Gall and Rim.²⁸ Briefly, the experimental apparatus was an electropolished stainless steel chamber (CTH-24, Eagle Stainless) in which flowrate, temperature, and humidity conditions were controlled to maintain environmental conditions. Air was supplied by laboratory compressed air supply and passed through a particle filter and granular activated carbon filter to remove particles and volatile organics in inlet air. Air was humidified to a setpoint by control of two flows, one passed through an impinging column filled with purified water and a second bypass flow. Ozone was injected into dry air (bypass flow) using a stable O₃ generator (97-0067-01, UVP). Chamber temperature was controlled by circulating the outflow of a temperature-controlled water bath

(Neslab RTE 10, Thermo Scientific) through vinyl tubing wrapped around the exterior surfaces of the chamber.

All flows were controlled and measured using mass flow controllers (GFC17A, Aalborg). Inlet and chamber temperature and relative humidity were measured via sensors (S-THB-M-002, Onset) inserted into the chamber inlet line and through a septum in a chamber access port, respectively; the sensor which protruded slightly into the chamber was included as part of the chamber background. Ozone was monitored using a UV absorbance federal equivalent method instrument (106-L, 2BTech). The chamber was operated at a flowrate of 1.88 L/min, and target conditions of inlet O₃, temperature, and relative humidity of 100 ppb, 22 °C, and 50% RH. Actual chamber conditions were (mean across all experiments ± 1 s.d.) 100.2 ± 5.2 ppb, 21.95 ± 0.91 °C and 50.9 ± 0.51% respectively. An inlet O₃ concentration of 100 ppb was chosen to represent a high, albeit realistic, outdoor O₃ concentration that exterior building enclosures are subjected to in a high ambient O₃ environment.

2.3 Volatile organic compound measurements

Primary emissions of volatile organic compounds (VOCs, primary emissions calculated in the absence of O₃) and byproduct formation yields (VOCs emitted due to O₃ surface flux) were calculated with established methods (Lamble et al.²⁹) using concentration data measured via proton transfer reaction – time of flight – mass spectrometry (PTR-TOF1000, Ionicon). The PTR-TOF-MS scanned across 17-250 amu for compounds with a proton affinity higher than that of H₂O. The drift tube conditions were 600 V, 60 °C, and 2.28 mbar. The PTR-TOF-MS was operated at an E/N value of 130. The mass axis was calibrated to three peaks: NO ($m/z = 29.9974$), C₃H₇O⁺ ($m/z = 59.0497$) and a C₆H₄I₂ fragment ($m/z = 203.944$) that was continuously injected into the drift tube via a heated permeation device (PerMaScal, Ionicon).

1
2
3 The PTR-TOF-MS inlet was maintained at 60 °C and the supplemental inlet flow to the drift
4 tube was 50 mL/min. Mass spectra were stored in 10 s intervals.
5
6
7
8
9

10 Compounds were first identified using a peak table resolved with unit mass resolution. This
11 method was selected given the limitations associated with the mass resolving power of the PTR-
12 TOF1000 ($m/\Delta m \sim 1000$). Ions known to be associated with instrument operation were removed
13 from the analysis (m/z 29, 30, 32, 34, 36, 37, 38, 39, 46, 50).³⁰ Compounds meeting a threshold
14 of statistically significant difference due to the material or material and O₃ presence (Section
15 2.5.3) are first identified according to their unit mass. For observed primary fluxes and yields,
16 the five largest contributors to flux or yield are assigned an exact mass from the measured mass,
17 determined from the centroid of the peak of interest by manual inspection of mass spectra (PTR-
18 MS Viewer 3.2.12, Ionicon). The five largest contributors to flux are discussed in terms of their
19 putative chemical identification (ID), determined from evaluation of potential chemical
20 formulas that may result in the exact mass of each signal, analysis for presence of expected
21 isotopes for a given chemical ID, and a review of the literature for compounds expected to be
22 emitted from test materials in the presence or absence of O₃.
23
24
25
26
27
28
29
30
31
32
33
34
35
36
37
38
39
40
41

42 Following assignment of the five largest fluxes or yields, the remaining mass was allocated into
43 groups based on unit mass by carbon and hydrogen containing compounds (C_xH_y) and
44 oxygenated compounds containing one (C_xH_yO) and two oxygen atoms (C_xH_yO₂). The
45 approach was similar to that of Inomata et al.³¹; compounds were classified by attribution of a
46 general chemical formula based on the known series of families of compounds across a range
47 of one to fifteen carbon atoms. Dienes (m/z 55 + 14n), aromatics (m/z 79 + 14n), and alkenes
48 (m/z 43 + 14n) were assigned to C_xH_y. The series m/z 43 + 14n may also represent unsaturated
49 aldehydes; only m/z 43, 57, 71, and 85 were assigned from this series based on manual
50
51
52
53
54
55
56
57
58
59
60

1
2
3 inspection of spectra for each compound at these m/z for each material tested. Assignment to
4
5 C_xH_y or C_xH_yO was based on the closest alignment of the exact mass and expected isotopes due
6
7 to presence or absence of oxygen. Saturated aldehydes and ketones (m/z $31 + 14n$), phenols (m/z
8
9 $95 + 14n$), and m/z 33 were assigned to C_xH_yO . Along the series m/z $47 + 14n$, mono- and di-
10
11 oxygenated compounds were distinguished by manual inspection of mass spectra for expected
12
13 isotopes from compounds containing two vs. one oxygen atoms and assigned to either C_xH_yO
14
15 or to $C_xH_yO_2$. All other compounds remained unidentified as “other” mass flux.
16
17
18
19
20

21
22 Volatile organic compounds were quantified with the PTR-TOF-MS using a relative
23
24 transmission method similar to methods described elsewhere.³² A transmission curve was
25
26 generated using eight calibration compounds spanning protonated mass of 33 to 135 (methanol,
27
28 1,3-butadiene, methyl vinyl ketone, benzene, toluene, *p*-xylene, 1,3,5-trimethyl benzene,
29
30 1,2,3,5-tetramethyl benzene). Calibration compounds were diluted to 100 ppb from an initial
31
32 nominal mixing ratio of 2 ppm from a compressed gas cylinder (Airgas) using a dilution system
33
34 that mixed a known flowrate of zero air (Airgas) with a known flowrate from the compressed
35
36 cylinder containing gas standards. The relative transmission method requires an estimate of the
37
38 mixing ratio of H_3O^+ isotope, typically approximated from the mass signal of the isotope at m/z
39
40 21.022. We determined this parameter using the generated transmission curve from the data
41
42 analysis software for the instrument (PTR-MS Viewer 3.2.12, Ionicon) and calculating a best-
43
44 fit value of transmission at m/z 21.022 that resulted in the minimization of the sum of squared
45
46 errors between the reported concentration of the eight compounds used in generation of
47
48 transmission curve and the known concentrations from the diluted calibration standard. Using
49
50 this method, reported concentrations for all compounds in the calibration curve were estimated
51
52 with the transmission method to within 20% of calibration value. For compounds present in the
53
54 calibration standard, reaction rate constants were taken from Zhao and Zhang.³³ For other
55
56
57
58
59
60

1
2
3 compounds, quantification was made using the transmission factor and the Ionicon default
4 reaction rate constant of $2 \times 10^{-9} \text{ cm}^3 \text{ s}^{-1} \text{ molecule}^{-1}$. After calculation via the transmission curve,
5
6 quantification of the five largest primary emission fluxes or yields was corrected for
7
8 isotopologues by correcting the major signal for its contribution to the total mass of the
9
10 compound.³⁴ Reported concentrations for the five largest primary emissions sources or sinks
11
12 and yields are corrected by manual inspection of peak assignment, correction for known isotopic
13
14 interferences when greater than 1%, and deconvolution of overlapping peaks where instrument
15
16 resolution is sufficient (e.g., separation of protonated methanol (m/z 33.0335) from one oxygen-
17
18 17 isotopologue of O_2^+ (m/z 32.9971)). These analyses were all performed in PTR-MS Viewer
19
20 3.2.12 (Ionicon).
21
22
23
24
25
26

27 *2.4 Experimental protocol*

28
29 Prior to initiation of experiments, the stainless-steel chamber surfaces and test material glass
30
31 enclosures were cleaned and passivated to reduce background reactions between O_3 and
32
33 chamber surfaces. The chamber and enclosures were first cleaned with water and soap and
34
35 rinsed three times. Surfaces were rinsed with reagent grade isopropyl alcohol followed by
36
37 methanol, followed by hexane (all compounds Sigma-Aldrich, 98% or greater purity). Surfaces
38
39 were allowed to dry in a fume hood overnight and were then heated with a heat gun. The day
40
41 before an experiment, the chamber was passivated by introducing elevated O_3 (>500 ppb) into
42
43 the chamber for at least 10 hours.
44
45
46
47
48
49

50 The experimental protocol included measurement of VOCs and O_3 levels in the inflow and
51
52 outflow of an empty chamber (background) before and after experiments where materials were
53
54 tested in the presence or absence of O_3 . Volatile organic compounds and O_3 levels were
55
56 measured at the chamber outlet or inlet following the timeline described in Figure 1. The
57
58 duration of each sample period was selected by calculation of the predicted time to reach steady-
59
60

state in a non-reactive chamber. It was calculated that an unreactive chamber would reach 99% of steady-state O₃ levels after ~30 minutes; surface reactions will reduce this time to reach steady-state. The steady-state condition was confirmed for each experiment by evaluating if chamber O₃ levels deviated more than 2 ppb in the final 20 minutes of each chamber monitoring period, a similar criteria to prior studies.³⁵ All experiments met the steady-state criteria for chamber O₃ levels. Following the completion of each experiment, the chamber was prepared for the next experiment by passivating the chamber overnight.

2.5 Data analysis

2.5.1 Quantification of volatile organic compound source and sink strength

Primary emissions of VOCs are those compounds emitted due to the presence of the material itself, and in the context of this study, in the absence of O₃. Primary emissions from the test samples were calculated according to equation 1:

$$E_{primary} = \frac{\lambda V(C_{i,outlet} - C_{i,inlet}) - \lambda V(C_{i,outlet,BG} - C_{i,inlet,BG}) \left(1 - \frac{A_e}{A_{BG}}\right)}{A_e} \quad (1)$$

where λ is the air exchange rate (s⁻¹), V is the volume of the stainless steel chamber (cm³), $C_{i,outlet}$ and $C_{i,inlet}$ are the concentrations of compound i in outlet and inlet chamber air with a test material present, respectively (ppb), $C_{i,outlet,BG}$ and $C_{i,inlet,BG}$ are the concentrations of compound i in outlet and inlet chamber air for an empty chamber test, respectively (ppb) and A_e and A_{BG} are the surface areas of the exposed sample and the stainless steel chamber, respectively (cm²).

The molar yield describes the amount of byproduct formed as a result of chemical reactions between a reactant, in this case O₃, and the material, normalized by the flux of O₃ to the

1
2
3 surface.³⁶ The molar yield was calculated following the method described by Lamble et al.,²⁹
4
5 shown in equation 2:

$$6 \quad Y_i = \frac{C_{i,outlet,O_3} - C_{i,outlet,o}}{C_{O_3,in} - C_{O_3,e}} \quad (2)$$

7
8
9
10
11 where Y_i is the molar yield of compound i (moles i formed/moles O_3 consumed, or mol/mol),
12
13 $C_{i,outlet,O_3}$ is the concentration of compound i following O_3 exposure, $C_{i,outlet,o}$ is the concentration
14
15 of compound i prior to O_3 exposure, $C_{O_3,in}$ is the concentration of O_3 at the chamber inlet, and
16
17 $C_{O_3,e}$ is the concentration of O_3 at the chamber outlet (ppb), corrected for losses to chamber
18
19 walls.
20
21
22

23 24 25 2.5.2 Ozone deposition

26
27 The deposition velocity (v_d) of a test material was calculated from measurement of inlet and
28
29 outlet O_3 levels from experiments conducted with an empty chamber and the chamber
30
31 containing a test material sample. The steady-state O_3 deposition velocity is calculated as
32
33 described previously³⁷ and shown in equation 3:
34
35

$$36 \quad v_d = \lambda \frac{V}{A_e} \left(\frac{C_{inlet}}{C_{outlet}} - 1 \right) - v_{d,BG} \frac{A_{BG}}{A_e} \quad (3)$$

37
38 where C_{inlet} and C_{outlet} represent the O_3 concentrations in the inlet and outlet air flow of the
39
40 chamber, respectively (ppb), and v_d and $v_{d,BG}$ are the O_3 deposition velocities for test material
41
42 and chamber, respectively (cm s^{-1}) and all other terms as described previously.
43
44
45
46
47
48
49

50 Background O_3 deposition velocities ($v_{d,BG}$) are calculated by performing an experiment with
51
52 an empty chamber for a fixed air exchange rate until steady-state O_3 concentrations are
53
54 achieved. Inlet and outlet concentrations of O_3 averaged over the final 20 minutes of data
55
56 collection are used to solve eq. 3 for $v_{d,BG}$ when $v_d = 0$ and there is no exposed test material area
57
58 (A_e). To measure the deposition velocity to the insulation material (v_d), the test procedure is
59
60

1
2
3 repeated for experiments with insulation materials placed in the chamber, and eq. 3 is solved
4
5 for the unknown values of v_d . An estimate of uncertainty was calculated using a propagation of
6
7 errors, incorporating uncertainties of the O₃ monitors of 2% of reading and flow controllers of
8
9 1.5%.

10
11
12
13
14 Ozone deposition was further parameterized by determining the material reaction probability
15
16 (γ , dimensionless), or the fraction of O₃ molecule-surface collisions that result in a reaction. To
17
18 calculate the reaction probability, the transport limited deposition velocity (v_t , cm/s) was first
19
20 determined by applying potassium iodide to surfaces using previously described protocols²⁷ and
21
22 γ was calculated using equation 4 as described by Cano-Ruiz et al. (1993)³⁸:

$$\gamma = \frac{4}{\langle v_b \rangle} \left(\frac{1}{v_d} - \frac{1}{v_t} \right)^{-1} \quad (4)$$

23
24
25 where $\langle v_b \rangle$ is the Boltzmann velocity, and is equal to 3.6110 cm/s for O₃ at 22°C.

26
27
28
29
30
31
32
33
34 As shown in Table 1, we determined the transport-limited deposition velocity experimentally
35
36 for four different materials. For materials for which v_t was not directly calculated, we assigned
37
38 a v_t value for the material with the most similar surface morphology (see Table 1), similar to
39
40 the approach taken by Lamble et al.²⁹ Uncertainty in reaction probabilities was calculated from
41
42 a propagation of errors from experiments conducted to determine $v_{d,BG}$, v_d , and v_t .

43 44 45 46 47 48 *2.5.3 Statistical testing for significant VOC emissions*

49
50 Data generated by the PTR-TOF-MS, when initially analysed with unit mass resolution,
51
52 resulted in time-series mass spectra with >200 peaks each. These spectra required subsequent
53
54 analysis for identification of peaks with significant differences due to material presence
55
56 (primary emissions) or material and O₃ presence (molar yield). For statistical testing to identify
57
58 primary emissions, we selected 100 steady-state time series data points from each of the test
59
60

1
2
3 conditions of empty chamber outlet and chamber with material outlet. Statistical significance
4
5 was determined by comparing datasets for each mass unit with a t-test with $\alpha = 0.05$.
6
7

8
9
10 For molar yields, comparisons required three groups: the empty chamber in the presence of O_3 ,
11
12 the chamber with only the material present, and the chamber with the material and O_3 present.
13
14 As with statistical testing for primary emissions, 100 steady-state time series data points were
15
16 selected for each of the three test conditions. Statistical testing required consideration of
17
18 multiple comparisons; thus, 3-group ANOVA was used to determine if statistically significant
19
20 differences existed across comparisons. The ANOVA F-Test was first calculated for each mass
21
22 signal to determine if at least two of the means across groups were significantly different. This
23
24 test was performed with $\alpha = 0.05$. If the F-Test determined at least two comparisons within the
25
26 three groups were different, a post-hoc Bonferroni-corrected t-test was performed for each of
27
28 the three possible combinations of t-tests between the groups. The Bonferroni correction
29
30 resulted in a p-value for the t-test statistic of 0.017. Yields were included as statistically
31
32 significant only if three conditions were met: 1) the F-Test met the significance threshold, 2) t-
33
34 test comparison between chamber with material and O_3 and empty chamber with O_3 met t-test
35
36 threshold, and 3) t-test comparison between chamber with material and O_3 and chamber with
37
38 only material present met t-test threshold.
39
40
41
42
43
44
45
46
47
48
49
50
51
52
53
54
55
56
57
58
59
60

3 RESULTS AND DISCUSSION

3.1 Primary emissions from building insulation materials

An example of the resulting estimation of molar fluxes across unit mass resolved mass spectra from the PTR-TOF-MS is shown in Figure 2 for cellulose and fiberglass. Note that these emissions were those determined from the presence of the material alone, i.e., in the absence of O₃. From Figure 3, it can be observed that cellulose emits a larger quantity and more diverse range of volatile organic compounds due to the material itself compared to fiberglass, expected given the organic nature of cellulosic material vs. the higher inorganic content present in the fiberglass material. Mass to charge ratios where no flux is reported are those m/z ratios where the comparison of the empty chamber to the chamber with material did not meet the statistical threshold for significance ($\alpha > 0.05$).

A summary of primary emission source and sink behaviour is shown in Figure 3 for all tested materials. Detailed tables showing mass accuracy, putative chemical ID, and additional notes can be found in the supporting information in Table S2. In general, the tested materials acted as a source of VOCs to the chamber outlet, although in some circumstances statistically significant decreases in chamber levels for specific VOCs compared to background tests were detectable for some materials. Note that for each statistically significant mass signal (see Section 2.5.3) from the PTR-TOF-MS, the compound was considered as a source if equation 1 was positive for that mass signal and a sink if equation 1 was negative. Thus, as shown in Figure 3, materials exhibit may act as a source for certain compounds while acting as a sink for others.

Cellulose insulation was the largest emitter of VOCs followed by recycled denim. Interestingly, both materials are made from recycled materials, as the cellulose was primarily derived from recycled newsprint. Cellulose is also one of the major components of denim,³⁹ explaining the similar magnitude and composition of observed primary VOC fluxes. PSTB, when subtracting

1
2
3 positive VOC fluxes (sources) from negative VOC fluxes (sinks), had the lowest VOC
4
5 emissions of all tested materials, due in part to the modest sink effect observed for compounds
6
7 m/z 47.0131, m/z 45.031, and m/z 61.0289 (see Table S2).
8
9

10
11 A thorough exploration of the potential chemical mechanisms impacting primary emissions for
12
13 each material is beyond the scope of this paper but may be warranted in the future given the
14
15 relatively high primary emissions observed here for some materials. In the case of cellulose, the
16
17 largest emitter, there exists a body of research demonstrating the instability of cellulose and
18
19 release of VOCs. As noted previously, cellulose is also a common recycled insulation material,
20
21 and is present in many other consumer products present indoors. For the five largest significant
22
23 fluxes from cellulose, we speculate that chemical assignments are protonated methanol
24
25 (CH_3OH), an acid fragment possibly associated with isopropyl alcohol,⁴⁰ acetaldehyde
26
27 ($\text{C}_2\text{H}_4\text{O}$), formic acid (CH_2O_2) and acetic acid (CH_3COOH). Note that because of the limitations
28
29 with the mass resolving power of the instrument and resulting potential for interferences, these
30
31 assignments should be taken as tentative chemical identifications.
32
33
34
35
36
37
38

39 Cellulose is known to be a reactive material, subject to a wide variety of degradation routes
40
41 including chemical, thermal, and radiation induced reaction routes;⁴¹ the largest primary
42
43 emissions from cellulose may be explained from a variety of cellulose degradation mechanisms.
44
45 Low molecular weight organic acids are known to be formed from degradation of
46
47 polysaccharide chains in cellulose materials, forming acetic acid and formic acid.⁴² Acetic acid
48
49 was the highest measured flux ($24.2 \mu\text{moles m}^{-2} \text{ h}^{-1}$) from cellulose insulation, and has been
50
51 observed as an emitted product from degradation of cellulose-containing museum materials.⁴³
52
53 Methanol and acetic acid have also been observed in FLEC cell studies of emissions from
54
55 various solid wood products.⁴⁴ Note that wood is typically on the order of 40-50% cellulose.⁴⁵
56
57 Acetaldehyde is a commonly identified indoor air pollutant;¹ the presence of acetaldehyde flux
58
59
60

1
2
3 from cellulose insulation may derive from aerobic microbial activity, possibly from the
4 oxidation of ethanol present as a solvent in adhesives.⁴⁶ The presence of ethanol in the material
5 is plausible as the cellulose insulation is made from recycled newsprint; inks contain a variety
6 of solvents including ethanol.⁴⁷ We attribute the peak at m/z 47 to formic acid and not ethanol
7 due to its alignment with the exact mass of formic acid (m/z 47.0128) and the presence of
8 isotopes of intensity and at exact masses (m/z 48.01611 and m/z 49.017) expected for formic
9 acid in the mass spectra. However, it is possible that volatile ethanol is present in our air sample
10 at relatively low mixing ratio but is not distinguishable from the formic acid peak. Furfural is a
11 known marker of cellulose degradation,⁴⁸ and has been detected previously with PTR-TOF-MS
12 at m/z 97.0287 (protonated parent compound) and m/z 62.0334 (fragment).⁴⁹ Both signals are
13 statistically significantly elevated in the cellulose mass spectra, and in combination total a flux
14 of $\sim 1.1 \mu\text{moles m}^{-2} \text{ h}^{-1}$ of furfural; or the 7th largest observed VOC flux.

15
16
17
18
19
20
21
22
23
24
25
26
27
28
29
30
31
32
33 Interestingly, polyurethane primary VOC emissions appeared similar to that of cellulose
34 containing materials (cellulose and recycled denim). Some polyurethane spray foams may
35 include cellulosic materials,⁵⁰ although the material safety data sheet (MSDS) for the
36 polyurethane spray foam material used here did not list cellulose as part of the composition.
37 There is limited data in the peer-reviewed literature on VOC emissions from polyurethane spray
38 foam; a NIST report using micro-chambers on four spray foams reported the largest chemicals
39 identified as 1,4-dioxane, 1,2-dichloropropane, 1,4-dimethyl piperazine; Tris-(1-chloro-2-
40 propyl) phosphate (TCPP) and 1,2-dichlorobenzene.⁵¹ These compounds appear not to have
41 been the largest five emitters in our sample, however, a statistically significantly elevated signal
42 was observed at the corresponding m/z ratios for 1,4-dioxane (exact mass = m/z 89.059706,
43 measured mass = 89.05157). At a flux of $0.15 \mu\text{moles m}^{-2} \text{ h}^{-1}$, 1,4-dioxane would be the 19th
44 largest VOC flux from this material. Other compounds were out of range of the PTR-TOF-MS
45
46
47
48
49
50
51
52
53
54
55
56
57
58
59
60

1
2
3 mass range (TCPP), not detected (1,4-dimethylpiperzine and 1,2-dichloropropane), or possibly
4 detected at very low fluxes (1,2-dichlorobenzene). However, three of the four spray foams
5 tested in the NIST study were sampled 5-24 months after spraying. In this work, we tested the
6 spray foam within 48 hours of spraying. Thus, we speculate that the major contributor to the
7 observed VOCs is a result of the blowing agents used (or B-side components of this do-it-
8 yourself spray foam kit), which may contain, e.g., formic acid.⁵² A NIST report notes that “a
9 wide range of aldehydes” were detected in spray foam samples from a test house, however, the
10 house was aged for 1.5 years and these compounds may have originated from other sources,
11 adsorbed to the spray foam, and subsequently desorbed during sampling.⁵³

12
13
14
15
16
17
18
19
20
21
22
23
24
25
26 Polyisocyanurate was characterized by substantial VOC emissions from m/z 41.038577 and m/z
27 42.033826. We speculate that m/z 41.038577 is protonated propyne (C_3H_4), likely a fragment
28 of a larger molecule based on prior studies in the literature.^{54,55} The signal at m/z 42 may also
29 be associated with acetonitrile in PTR-MS studies;⁵⁶ the exact mass of acetonitrile aligned well
30 with the measured mass and acetonitrile is a solvent which may be used in the production of
31 polyisocyanate polymers.⁵⁷ However, it is also possible that this signal represents the fragment
32 of propanal.⁵⁸ Other materials (polystyrene, fiberglass, stonewool, PSTB) had generally lower
33 primary VOC emissions. Polystyrene was the only material with a large peak at m/z 105.0699,
34 which we attribute to styrene.

35
36
37
38
39
40
41
42
43
44
45
46
47
48
49 On a mass basis, total primary VOC emissions summed for all statistically significant unit
50 masses yields a total VOC (TVOC) mass flux ranging from $\sim 0.3 \text{ mg m}^{-2} \text{ h}^{-1}$ (from PSTB) to
51 $\sim 3.3 \text{ mg m}^{-2} \text{ h}^{-1}$ (from cellulose). These estimates are based on the summation of statistically
52 significantly elevated molar fluxes, assuming that the molecular weight of each compound is
53 one amu less than the protonated mass. The complete list of statistically significant positive
54
55
56
57
58
59
60

1
2
3 molar and estimated mass fluxes for cellulose and PSTB is available in Table S3. These
4
5 estimates of summed TVOC emissions are within the range of TVOC emissions reported for
6
7 many polymeric building materials; for example, TVOC emissions from plywood have been
8
9 shown to range 0.04-1.5 mg m⁻² h⁻¹.^{59,60} To explore the potential implications of these primary
10
11 TVOC fluxes, consider a well-mixed 150 m² single-story home with 3 m height walls and
12
13 dimensions of 10 m x 15 m. The total wall enclosure assembly area would be ~150 m². If
14
15 windows contribute 20% of the wall enclosure area, the total wall area would be ~120 m².
16
17 Assuming ~90% of the wall cavity is filled with the tested insulation materials (10% accounting
18
19 for studs and other construction elements), and that approximately half of the wall assembly
20
21 contributes VOC fluxes directly to the interior of the space (e.g., if stack-driven flow dominates
22
23 and leakage areas are evenly distributed along the vertical height, half would be a reasonable
24
25 approximation⁶¹), the TVOC flux from the wall cavity could contribute between ~16 mg/h and
26
27 ~180 mg/h, depending on material (and assuming mass transfer characteristics are consistent
28
29 between the cavity and the chamber test conditions; a useful but somewhat unrealistic
30
31 approximation). If the air exchange rate in the space is 0.5 h⁻¹, the resulting TVOC concentration
32
33 would be between ~70 µg/m³ and ~800 µg/m³. These approximations are reasonably consistent
34
35 with limited prior estimates of the contribution of wall cavity materials to indoor spaces of
36
37 which we are aware.^{9,11} However, future work beyond the scope defined herein should integrate
38
39 these findings into more mechanistic models of emissions and transport from enclosures to
40
41 interior spaces.
42
43
44
45
46
47
48
49

50 *3.2 Ozone removal to materials*

51
52 Results of the calculation of deposition velocity and reaction probability are presented in Figure
53
54 4. Ozone deposition tests were conducted in duplicate; error bars shown in Figure 4 are the
55
56 larger of propagated uncertainty or the range across duplicate tests. Results show that γ varied
57
58 by more than an order of magnitude across materials, from $\sim 1 \times 10^{-6}$ to $\sim 3 \times 10^{-5}$. These values
59
60

1
2
3 are in the range that Liu and Nazaroff¹⁵ predict could yield highly varying O₃ penetration factors
4 through insulation materials alone under realistic pressure differences, ranging from ~70%
5 penetration to <10% penetration.
6
7
8
9

10
11
12 There exist relatively few measurements of O₃ reactivity of building enclosure insulation
13 materials in the literature. To the best of our knowledge, reaction probabilities have been
14 reported only for fiberglass materials, which is discussed subsequently. Given the recent
15 acknowledgement that building envelopes can act as a protective barrier for O₃,^{21,62,63} we expect
16 these data to be useful for modelling indoor-outdoor O₃ transport and as an aid in building
17 enclosure material selection. In general, fibrous and loose materials (cellulose, fiberglass, stone
18 wool and recycled denim) appeared to have generally higher γ while rigid, smoother materials
19 (polyurethane, polystyrene, polyisocyanurate, and polystyrene with thermal backing (PSTB))
20 appeared to have lower γ . Given that estimates reported here are “effective” reaction
21 probabilities, meaning they are derived from a deposition velocity parameterized to horizontal
22 projections of test material surface area, these values are over-predictions relative to estimates
23 that consider the internal surface area of a material.⁶⁴ As will be discussed, this consideration is
24 of particular importance given the potential for complex and varied flow paths across or through
25 materials in building enclosure assemblies.
26
27
28
29
30
31
32
33
34
35
36
37
38
39
40
41
42
43
44
45
46

47 We measured the transport-limited deposition velocity for four materials, selecting materials
48 that varied in structure and morphology. Measured v_t are reported in Table S4 of the supporting
49 information, and ranged from 0.14 – 0.27 cm/s, indicating potential for transport of O₃ to the
50 surface to impact overall ozone removal for some tested materials. For the chamber conditions
51 used, resistance due to transport and surface reaction were on the same order of magnitude for
52 five of eight tested materials (PU, DM, SW, C, FG) while for three tested materials (PI, PSTB,
53
54
55
56
57
58
59
60

1
2
3 PS) the surface resistance dominated. Implications for uncertainty in calculated reaction
4 probabilities are discussed the supporting information.
5
6
7
8
9

10 As described in Sections 2.1-2.2, materials were tested in a well-mixed continuous flow reactor
11 (CFR) with one surface of the material prepared to allow interaction with the bulk chamber air.
12 The parameterization of the deposition velocity requires a surface area for calculation, normally
13 taken to be the horizontal projection of surface area. Air transport across or through materials
14 within building enclosures is complex, but it is expected that the majority of transport occurs
15 through pressure-driven flow across larger (0.2 - 1 mm in crack height) size cracks and gaps in
16 the enclosure.¹⁵ Liu and Nazaroff¹⁵ discuss the likely flow paths of air entering a building
17 enclosure filled with fiberglass insulation and conclude the airflows are likely to either traverse
18 through a fiberglass mat in the direction orthogonal to a vertical wall or bypass insulation in the
19 air space between the insulation and the frame. In the former case, it is likely that a fibrous mat
20 acts as filter, with greater internal surface area available for interaction than in the latter case of
21 airflow predominantly passing through void space.
22
23
24
25
26
27
28
29
30
31
32
33
34
35
36
37
38
39

40 Reaction probabilities calculated here are more likely to be representative of a scenario where
41 air movement occurs in the void space adjacent to a material in a two-phase material-air system.
42 While limited data exists reporting O₃ reaction probabilities to building insulation materials,
43 Liu and Nazaroff¹⁵ empirically estimate the reaction probability of fiberglass fibers to be 6×10^{-6} ,
44 lower than the value of 2.8×10^{-5} reported here. Note that the comparison of these reaction
45 probabilities is for that of a fiber of fiberglass compared to the effective reaction probability
46 made using a horizontally projected area of a material sample. In contrast, the reaction
47 probability reported here is similar to the value of $\sim 3 \times 10^{-5}$ reported by Lamble et al.²⁹ for
48 fiberglass ceiling tiles tested in a similar manner to the apparatus used in the present study. Liu
49
50
51
52
53
54
55
56
57
58
59
60

1
2
3 and Nazaroff⁵ use a plug flow reactor, described in detail by Morrison and Nazaroff,⁶⁵ that
4
5 exposes a greater internal surface area of the material to O₃-laden flow than the continuous flow
6
7 reactor (CFR) type apparatus used here and in Lamble et al.²⁹. Future studies of pollutant
8
9 transport and transformation occurring in building enclosures should carefully consider the
10
11 formulation, and assumptions inherent to, surface and transport resistance terms, as flow paths
12
13 in building enclosures are likely complex and both spatially and temporally variant.
14
15
16
17
18

19 *3.3 Ozone byproduct yields from building insulation materials*

20
21 Major contributors to the O₃ byproduct yield with the tested materials appear to be oxygenated
22
23 VOCs, primarily aldehydes; O₃ byproduct yields are shown in Figure 5. Yields ranged from
24
25 0.25 (polystyrene) to 0.85 (recycled denim) moles of byproduct formed per mole of O₃
26
27 consumed (mol/mol). For the experiments conducted here, these yields are equivalent to
28
29 secondary fluxes that range from 0.71 (polystyrene) to 10 (recycled denim) μmoles/m²/h. While
30
31 lower in magnitude than the primary emissions discussed in the scaling analysis in section 3.1,
32
33 it is plausible that secondary products from O₃ reactions on wall cavity materials could impact
34
35 indoor air quality. We believe these findings compel further study of the oxidation pathways in
36
37 wall cavities, including coupling of outdoor-enclosure-indoor fluid dynamics models with
38
39 studies of emissions and transformation.
40
41
42
43
44
45
46

47 Detailed tables showing mass accuracy, putative chemical ID, and additional notes for
48
49 compounds contributing significantly to the byproduct yield can be found in the supporting
50
51 information in Table S5. Buhr et al.⁵⁸ showed that most aldehydes will lose a molecule of water
52
53 leading to a main fragment at m/z (MH⁺ - 18). Therefore, we attribute the peak at m/z 83 to a
54
55 fragment of hexanal with a loss of a molecule of water (mass measured = 83.0804), consistent
56
57 with the presence of a peak at m/z 101 possibly corresponding to the protonated parent
58
59
60

1
2
3 compound. For the same reason, we also attribute the peak at m/z 55 to a fragment of butanal
4
5 (MH⁺ - 18) (exact mass = 55.054227, measured mass = 55.0454), confirmed by the presence of
6
7 a peak at m/z 73 corresponding to protonated parent compound (exact mass = 73.06534,
8
9 measured mass = 73.0411). However, this assignment should be taken with caution, as
10
11 fragmentation of hexanal can lead to a signal at m/z 55, which may also be true of heptanal
12
13 (Buhr et al, 2002). The presence of heptanal was also confirmed by the presence of a peak at
14
15 m/z 97, which corresponds to a loss of water from the parent compound as well. Aldehyde
16
17 fragments were found in cellulose, polyisocyanurate, fiberglass and stone wool insulation as
18
19 well as recycled denim insulation, although the hexanal fragment (m/z 83) was not among
20
21 statistically significant compounds for recycled denim.
22
23
24
25
26
27

28 Further limitations include the potential for presence of the structural isomers, such as propanal
29
30 and acetone as oxygenated byproducts from reaction of the materials with O₃. Mass signals at
31
32 m/z 59 were present for all materials. Only recycled denim and polyurethane contained
33
34 significant signals at m/z 41, although at higher levels than would be expected due to
35
36 fragmentation from a propanal parent at m/z 59. Thus, we conclude that for recycled denim and
37
38 polyurethane, both acetone and propanal are likely present in the sampled air. Given the
39
40 precedence for O₃-building material interactions to result in the formation of carbonyl
41
42 compounds and acetone,⁶⁶ this finding is expected. The PTR-TOF-MS method does not enable
43
44 the separation of these structural isomers, and so assignment of these compounds to signals in
45
46 a matrix possibly containing both compounds is challenging.
47
48
49
50
51

52 Interestingly, cellulose appears to have a different secondary emission profile and yield from
53
54 that of recycled denim although they had similar magnitude and composition of primary
55
56 emissions. This is most likely due to differences in material or surface-bound chemical
57
58
59
60

1
2
3 composition of the two materials, leading to different heterogenous chemistry that yields
4
5 distinct oxygenated products. The largest byproduct yield for cellulose corresponds mainly to
6
7 aldehyde fragments ($m/z = 55, 69$ and 83), acetone, and more widely to un-attributed mono- or
8
9 di-oxygenated compounds.
10

11
12
13 Heterogeneous reactions of recycled denim and polyurethane with O_3 led to high formation
14
15 yields for acetaldehyde (with contributions of acetaldehyde - water cluster at $m/z = 63.05$
16
17 according to Herbig et al.⁶⁷), acetone, and, more generally, mono- and di-oxygenated
18
19 compounds (~ 0.85 and ~ 0.53 mol/mol consumed for denim and polyurethane, respectively),
20
21 making them the highest emitters of byproducts in the presence of O_3 . Recycled denim and
22
23 polyurethane had similar yield profiles. A peak at $m/z 41$ likely corresponds to a propanal
24
25 fragment, pentanal fragment, and/or alcohol fragment according to Wyche et al.⁶⁸ (exact mass
26
27 = 41.038577 , measured mass = 41.0358). This peak was observed only for denim and
28
29 polyurethane with a yield of 0.05 mol/mol for both materials and could be related to the
30
31 oxidation of polyols present in polyurethane (polyols react in excess with isocyanates to make
32
33 polyurethane and can still be present in the final polymer and give aldehydes that react with O_3
34
35 and could lead to carboxylic acid in presence of water). A peak at $m/z 62$ was found as a
36
37 byproduct only in those two materials with relatively high yields (0.07 and 0.04 mol/mol for
38
39 denim and polyurethane, respectively). We attributed this peak to the protonated carbamic acid
40
41 (CH_3NO_2) due to its alignment with the exact mass (exact mass = 62.023655 , measured mass =
42
43 62.0266). The formation of those compounds with only those two materials in the presence of
44
45 O_3 might be explained by the presence of polyurethane in denim, which could explain the
46
47 similar composition in VOCs primary emission and byproducts formation.
48
49

50
51
52 Formic acid (exact mass = 47.012756 , measured mass = 47.0128) was common and one of the
53
54 most elevated yields among five of the eight materials (present in fiberglass, stone wool,
55
56 polyisocyanurate, polystyrene, and PSTB). Yield values ranged from 0.04 to 0.16 mol/mol.
57
58
59
60

1
2
3 Polyisocyanurate, fiberglass, and stone wool had a similar profile of byproduct formation yield,
4 with aldehyde fragments (for a total of 0.08, 0.09, and 0.08 mol/mol, respectively), formic acid
5 (0.06, 0.04, and 0.06 mol/mol, respectively), and acetone (0.05, 0.07, and 0.13 mol/mol,
6 respectively), with stone wool presenting a relatively high yield of acetaldehyde (0.06 mol/mol).
7
8 Polystyrene and PSTB had a very similar profile, with higher yields for formic acid, acetone,
9 and acetic acid with PSTB.
10
11
12
13
14
15
16
17
18

19 When considering both the removal of O₃ and the resulting byproduct formation yield, there
20 exists a range of behaviors. In general, O₃ reactivity does not appear to be predictive of
21 byproduct formation yield. Both cellulose and fiberglass have shown relatively high O₃ sink
22 strengths compared to the other materials tested in this study, but their secondary TVOC
23 formation rate is lower than other insulation materials. A potential reason for this is the cellulose
24 and fiberglass surface compounds may be structured to allow for a catalytic decomposition
25 pathway for O₃, resulting in the production of CO₂ and O₂. Recycled denim and polyurethane
26 appear to have the opposite behavior. Lower deposition velocities were found for these two
27 materials as compared to cellulose, but a higher formation yield was detected. Due to the fact
28 that they have similar primary emission profiles as cellulose, the difference is most likely due
29 to differences in surface morphology and the composition of these materials.
30
31
32
33
34
35
36
37
38
39
40
41
42
43

44 *3.4 Limitations and future work*

45
46 The work presented here represents, to our knowledge, a substantial expansion of the ozone
47 reactivity and primary and secondary emission behavior of building insulation materials.
48
49 However, there exist important sources of uncertainty in this investigation that compel future
50 studies of this important class of building material. First, while we selected eight materials to
51 span a range of commonly used insulation materials, there exist other types of wall enclosure
52 products that should be tested. In addition, there are multiple manufacturers of any given type
53
54
55
56
57
58
59
60

1
2
3 of insulation material, and variation in VOC emissions and ozone chemistry of a material type
4
5 for any given manufacturer is also possible. Future work could investigate variability among
6
7 similar products across different manufacturers as well as within-manufacturer variability (e.g.,
8
9 subsampling across a single lot of material as well as acquiring samples from a single
10
11 manufacturer with different manufacture dates).
12
13
14
15
16

17 The scope of this study was to investigate the VOC emissions and ozone reactivity of common
18
19 building insulation materials, as manufactured. Future work would also be well-served by
20
21 conducting additional characterization of materials to quantitatively capture differences in
22
23 material chemical composition and morphology. These data would advance understanding of
24
25 the drivers of observed differences in emission and reactivity behavior across materials. Primary
26
27 emissions were measured over a period of 55 minutes, ideally, emissions would be measured
28
29 over a longer time period to ensure full desorption of compounds that may have adsorbed to the
30
31 material from other sources (e.g., air in storage warehouse or in sample storage bag air). We
32
33 attempted to minimize this source of error by keeping materials in their manufactured bags and
34
35 limiting the amount of time the samples were exposed to laboratory air. Finally, while ionization
36
37 via PTR-TOF-MS is, in theory, “soft”, fragmentation of aldehydes is known phenomena that
38
39 complicates the calculation of emission rates of this class of compounds. Furthermore, the PTR-
40
41 TOF-MS is not a universal detector, future studies should inter-compare emission rates
42
43 estimated with PTR-TOF-MS complemented by, and in comparison with, other analytical
44
45 methods such as TD-GC-MS and HPLC-UV.
46
47
48
49
50
51
52

53 **4 CONCLUSIONS**

54
55 This study investigated the primary emissions, ozone (O₃) reactivity, and O₃ reaction byproduct
56
57 emissions from eight commonly used building insulation materials. Results demonstrate that
58
59
60

1
2
3 cellulose insulation was the largest emitter of primary VOCs, followed by recycled denim.
4
5 Polystyrene, fiberglass, and stone wool had relatively low primary VOC emissions, and
6
7 polystyrene with thermal backing actually served as a sink for some VOCs. The O₃ reaction
8
9 probability of these materials ranged more than an order of magnitude, and total reaction
10
11 byproduct yields ranged from ~0.25 to ~0.85 moles of byproduct formed per mole of O₃
12
13 consumed. A number of secondary VOCs resulting from O₃ reactions were logically deduced
14
15 (and varied by material), but further analysis should be done to clearly identify the secondary
16
17 byproducts formed due to oxidation of insulation. To our knowledge, this study provides the
18
19 first characterization of the aforementioned parameters for a range of common insulation
20
21 materials. The data presented herein could serve as the basis for informing quantitative
22
23 comparisons of trade-offs between different enclosure insulation materials, e.g., consideration
24
25 of thermal resistance in conjunction with material emissions, O₃ removal, and byproduct
26
27 formation. These data can also inform building enclosure transport modelling efforts, which we
28
29 recommend be improved upon in future work to incorporate the ability to predict the impacts
30
31 of oxidation chemistry in building enclosures on both primary and secondary pollutant fluxes
32
33 into the space.
34
35
36
37
38
39
40

41 **ACKNOWLEDGEMENT**

42
43 ETG was supported by start-up funds from the Portland State University College of
44
45 Engineering. This material is based in part upon work supported by the National Science
46
47 Foundation under Grant No. 1560383. BS was partially supported by an ASHRAE New
48
49 Investigator Award.
50
51
52

53 **5 REFERENCES**

- 54
55 1 J. M. Logue, T. E. McKone, M. H. Sherman and B. C. Singer, *Indoor Air*, 2011, **21**, 92–109.
56 2 C. J. Weschler, *Indoor Air*, 2000, **10**, 269–288.
57 3 M. L. Bell, A. McDermott, S. L. Zeger, J. M. Samet and F. Dominici, *J. Am. Med. Assoc.*,
58 2004, **292**, 2372–2378.
59
60

- 1
- 2
- 3
- 4 M. Jerrett, R. T. Burnett, C. A. Pope, K. Ito, G. Thurston, D. Krewski, Y. Shi, E. Calle and M. Thun, *N. Engl. J. Med.*, 2009, **360**, 1085–1095.
- 5 J. I. Levy, S. M. Chemerynski and J. A. Sarnat, *Epidemiology*, 2005, **16**, 458–468.
- 6 J. F. Gent, E. W. Triche, T. R. Holford, K. Belanger, M. B. Bracken, W. S. Beckett and B. P. Leaderer, *JAMA J. Am. Med. Assoc.*, 2003, **290**, 1859–1867.
- 7 J. L. Peel, M. Klein, W. D. Flanders, J. A. Mulholland, G. Freed and P. E. Tolbert, *Environ. Health Perspect.*, 2011, **119**, 1321–1327.
- 8 N. Fann, A. D. Lamson, S. C. Anenberg, K. Wesson, D. Risley and B. J. Hubbell, *Risk Anal. Off. Publ. Soc. Risk Anal.*, 2012, **32**, 81–95.
- 9 D. E. Hun, M. C. Jackson and S. S. Shrestha, *Optimization of Ventilation Energy Demands and Indoor Air Quality in the ZEB Alliance Homes*, Oak Ridge National Laboratory, Oak Ridge, TN, 2013.
- 10 C. Hachem, P. Fazio, J. Rao, K. Bartlett and Y. P. Chaubey, *Build. Environ.*, 2009, **44**, 1691–1698.
- 11 H. Li, M. Yang, J. S. Zhang and M. Salonvaara, *ASHRAE Trans.*, 2005, **111**, 210–217.
- 12 W. R. Chan, W. W. Nazaroff, P. N. Price, M. D. Sohn and A. J. Gadgil, *Atmos. Environ.*, 2005, **39**, 3445–3455.
- 13 M. Ji, D. S. Cohan and M. L. Bell, *Environ. Res. Lett. ERL Web Site*, , DOI:10.1088/1748-9326/6/2/024006.
- 14 M. Yan, Z. Liu, X. Liu, H. Duan and T. Li, *Chemosphere*, 2013, **93**, 899–905.
- 15 D.-L. Liu and W. W. Nazaroff, *Atmos. Environ.*, 2001, **35**, 4451–4462.
- 16 C. J. Weschler, *Environ. Health Perspect.*, 2006, **114**, 1489–1496.
- 17 M. S. Waring, *Indoor Air*, 2014, **24**, 376–389.
- 18 C. Chen, B. Zhao and C. J. Weschler, *Environ. Health Perspect.*, 2012, **120**, 235–240.
- 19 I. S. Walker, M. H. Sherman and W. W. Nazaroff, *Ozone Reductions Using Residential Building Envelopes*, California Energy Commission, PIER Energy-Related Environmental Research Program, 2010.
- 20 I. S. Walker and M. H. Sherman, *Build. Environ.*, 2013, **59**, 456–465.
- 21 B. Stephens, E. T. Gall and J. A. Siegel, *Environ. Sci. Technol.*, 2012, **46**, 929–936.
- 22 H. Zhao and B. Stephens, *Indoor Air*, 2016, **26**, 571–581.
- 23 C. J. Weschler, *Atmos. Environ.*, 2004, **38**, 5715–5716.
- 24 C. J. Weschler, *Indoor Air*, 2004, **14 Suppl 7**, 184–194.
- 25 G. Morrison, *Curr. Sustain. Energy Rep.*, 2015, **2**, 33–40.
- 26 C. J. Weschler, *Indoor Air*, 2011, **21**, 205–218.
- 27 E. T. Gall, R. L. Corsi and J. A. Siegel, *Environ. Sci. Technol.*, 2014, **48**, 3682–3690.
- 28 E. T. Gall and D. Rim, *Build. Environ.*, 2018, **138**, 89–97.
- 29 S. P. Lamble, R. L. Corsi and G. C. Morrison, *Atmos. Environ.*, 2011, **45**, 6965–6972.
- 30 A. Vlasenko, J. G. Slowik, J. W. Bottenheim, P. C. Brickell, R. Y.-W. Chang, A. M. Macdonald, N. C. Shantz, S. J. Sjostedt, H. A. Wiebe, W. R. Leitch and J. P. D. Abbatt, *J. Geophys. Res. Atmospheres*, , DOI:10.1029/2009JD012025.
- 31 S. Inomata, H. Tanimoto, Y. Fujitani, K. Sekimoto, K. Sato, A. Fushimi, H. Yamada, S. Hori, Y. Kumazawa, A. Shimono and T. Hikida, *Atmos. Environ.*, 2013, **73**, 195–203.
- 32 R. Holzinger, A. Kasper-Giebl, M. Staudinger, G. Schauer and T. Röckmann, *Atmospheric Chem. Phys.*, 2010, **10**, 10111–10128.
- 33 J. Zhao and R. Zhang, *Atmos. Environ.*, 2004, **38**, 2177–2185.
- 34 C. Sarkar, V. Sinha, V. Kumar, M. Rupakheti, A. Panday, K. S. Mahata, D. Rupakheti, B. Kathayat and M. G. Lawrence, *Atmospheric Chem. Phys.*, 2016, **16**, 3979–4003.
- 35 B. K. Coleman, M. M. Lunden, H. Destailats and W. W. Nazaroff, *Atmos. Environ.*, 2008, **42**, 8234–8245.
- 36 G. C. Morrison and W. W. Nazaroff, *Environ. Sci. Technol.*, 2002, **36**, 2185–2192.

- 1
2
3 37 O. A. Abbass, D. J. Sailor and E. T. Gall, *Atmos. Environ.*, 2017, **148**, 42–48.
- 4 38 J. A. Cano-Ruiz, D. Kong, R. B. Balas and W. W. Nazaroff, *Atmos. Environ.*, 1993, **27**,
5 2039–2050.
- 6 39 A. Kumari and K. Khurana, Regenerated Cellulose-Based Denim Fabric for Tropical
7 Regions, <https://www.hindawi.com/journals/jtex/2016/4614168/>, (accessed November 26,
8 2018).
- 9 40 N. Hayeck, B. Temime-Roussel, S. Gligorovski, A. Mizzi, R. Gemayel, S. Tlili, P. Maillot,
10 N. Pic, T. Vitrani, I. Poulet and H. Wortham, *Int. J. Mass Spectrom.*, 2015, **392**, 102–110.
- 11 41 M. C. Area and H. Cheradame, *BioResources*, 2011, **6**, 5307–5337–5337.
- 12 42 H. Kraessig, *J. Polym. Sci. Part C Polym. Lett.*, 1987, **25**, 87–88.
- 13 43 M. Strlič, I. K. Cigić, J. Kolar, G. De Bruin and B. Pihlar, *Sensors*, 2007, **7**, 3136–3145.
- 14 44 M. Risholm-Sundman, M. Lundgren, E. Vestin and P. Herder, *Holz Als Roh- Werkst.*, 1998,
15 **56**, 125–129.
- 16 45 R. C. PETERSEN, in *The Chemistry of Solid Wood*, American Chemical Society, 1984,
17 vol. 207, pp. 57–126.
- 18 46 S. Tohmura, A. Ishikawa, K. Miyamoto and A. Inoue, *J. Wood Sci.*, 2012, **58**, 57–63.
- 19 47 United States, US8110031B2, 2012.
- 20 48 T. Łojewski, T. Sawoszczuk, J. M. Łagan, K. Zięba, A. Barański and J. Łojewska, *Appl.*
21 *Phys. A*, 2010, **100**, 873–884.
- 22 49 T. M. Ruuskanen, M. Müller, R. Schnitzhofer, T. Karl, M. Graus, I. Bamberger, L. Hörtnagl,
23 F. Brilli, G. Wohlfahrt and A. Hansel, *Atmospheric Chem. Phys.*, 2011, **11**, 611–625.
- 24 50 J. L. Rivera-Armenta, T. Heinze and A. M. Mendoza-Martínez, *Eur. Polym. J.*, 2004, **40**,
25 2803–2812.
- 26 51 D. G. Poppendieck, M. Gong and L. E. Lawson, .
- 27 52 GTZ Proklima, *Natural Foam Blowing Agents*, Federal Ministry for Economic Cooperation
28 and Development (BMZ), Environment and Sustainable Use of Natural Resources Division,
29 2012.
- 30 53 D. G. Poppendieck, M. Gong and S. J. Emmerich, *Tech. Note NIST TN - 1921*.
- 31 54 E. A. Bruns, J. G. Slowik, I. E. Haddad, D. Kilic, F. Klein, J. Dommen, B. Temime-Roussel,
32 N. Marchand, U. Baltensperger and A. S. H. Prévôt, *Atmospheric Chem. Phys.*, 2017, **17**,
33 705–720.
- 34 55 T. Maihom, E. Schuhfried, M. Probst, J. Limtrakul, T. D. Märk and F. Biasioli, *J. Phys.*
35 *Chem. A*, 2013, **117**, 5149–5160.
- 36 56 E. Dunne, I. E. Galbally, S. Lawson and A. Patti, *Int. J. Mass Spectrom.*, 2012, **319–320**, 40–
37 47.
- 38 57 U.S. Patent and Trademark Office, US06225934, 1981.
- 39 58 K. Buhr, S. van Ruth and C. Delahunty, *Int. J. Mass Spectrom.*, 2002, **221**, 1–7.
- 40 59 C. Yu and D. Crump, *Build. Environ.*, 1998, **33**, 357–374.
- 41 60 Y.-H. Cheng, C.-C. Lin and S.-C. Hsu, *Build. Environ.*, 2015, **87**, 274–282.
- 42 61 I. S. Walker and D. J. Wilson, *HVACR Res.*, 1998, **4**, 119–139.
- 43 62 Z. Gao and J. S. Zhang, *HVACR Res.*, 2012, **18**, 160–168.
- 44 63 D. Lai, P. Karava and Q. Chen, *Build. Environ.*, 2015, **93**, 112–118.
- 45 64 E. T. Gall, J. A. Siegel and R. L. Corsi, *Environ. Sci. Technol.*, 2015, **49**, 4398–4406.
- 46 65 G. C. Morrison and W. W. Nazaroff, *Environ. Sci. Technol.*, 2000, **34**, 4963–4968.
- 47 66 E. Gall, E. Darling, J. A. Siegel, G. C. Morrison and R. L. Corsi, *Atmos. Environ.*, 2013, **77**,
48 910–918.
- 49 67 J. Herbig, T. Titzmann, J. Beauchamp, I. Kohl and A. Hansel, *J. Breath Res.*, 2008, **2**,
50 037008.
- 51 68 K. P. Wyche, R. S. Blake, A. M. Ellis, P. S. Monks, T. Brauers, R. Koppmann and E. C.
52 Apel, *Atmospheric Chem. Phys.*, 2007, **7**, 609–620.
- 53
54
55
56
57
58
59
60

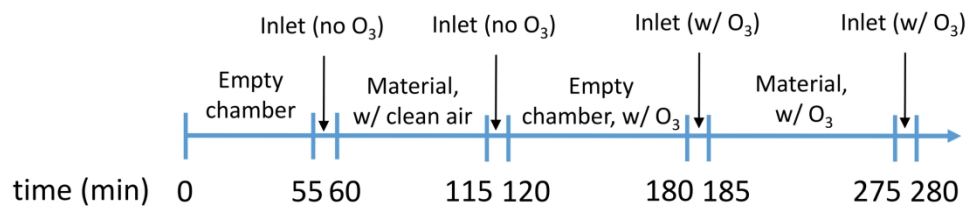
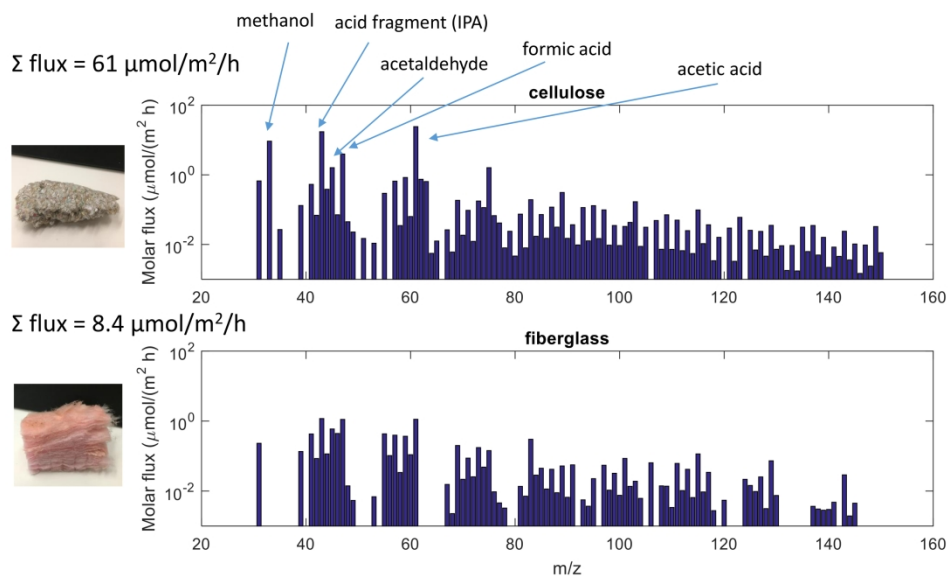


Figure 1. Summary of experimental protocol for testing of ozone reaction probabilities, primary emissions of volatile organic compounds and byproduct formation yields.

196x47mm (300 x 300 DPI)



25
26
27
28
29

Figure 2. Example of unit mass resolution spectra for calculation of primary emission fluxes from cellulose and fiberglass across m/z 20-160. Putative chemical identification is shown for cellulose based on further analysis of exact mass, isotopic ratio, and survey of the literature for likely compounds emitted from the material.

30
31
32
33
34
35
36
37
38
39
40
41
42
43
44
45
46
47
48
49
50
51
52
53
54
55
56
57
58
59
60

247x143mm (300 x 300 DPI)

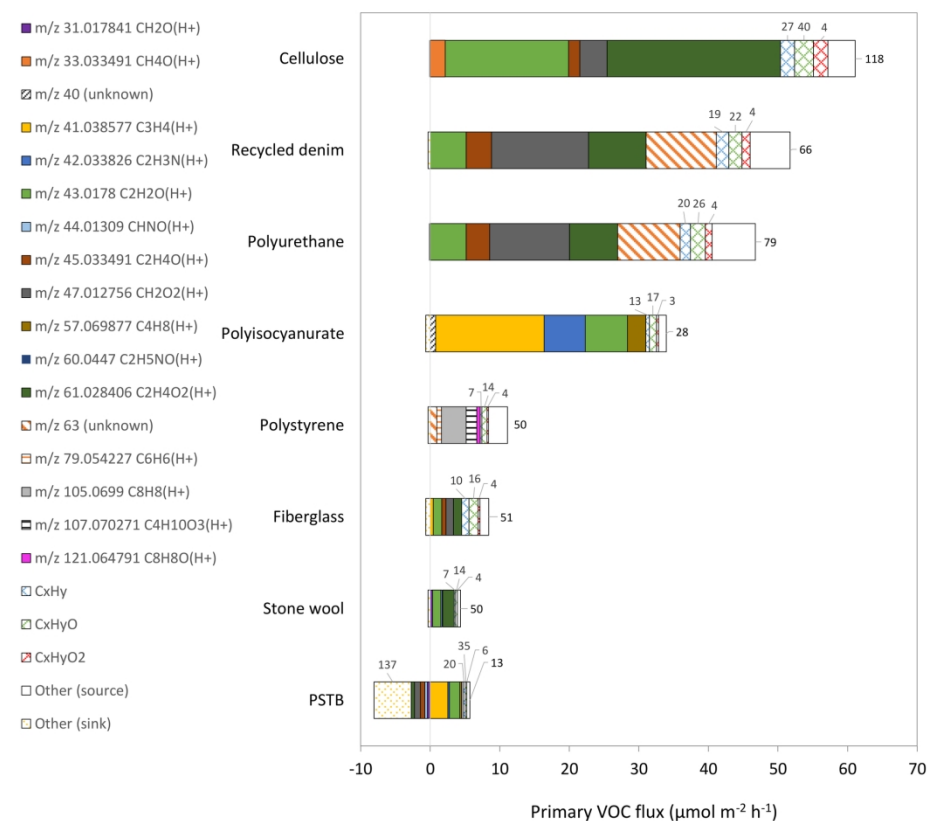


Figure 3. Summary of primary emissions of volatile organic compound sources and sinks for each material. Note that the data labels on the C_xH_y , $\text{C}_x\text{H}_y\text{O}$, $\text{C}_x\text{H}_y\text{O}_2$, and Other categories refer to the number of unique, statistically significantly elevated compounds identified in the comparison of the empty chamber to the chamber with a material present. These compounds were identified with unit mass resolution. PSTB = polystyrene with thermal backing.

180x154mm (300 x 300 DPI)

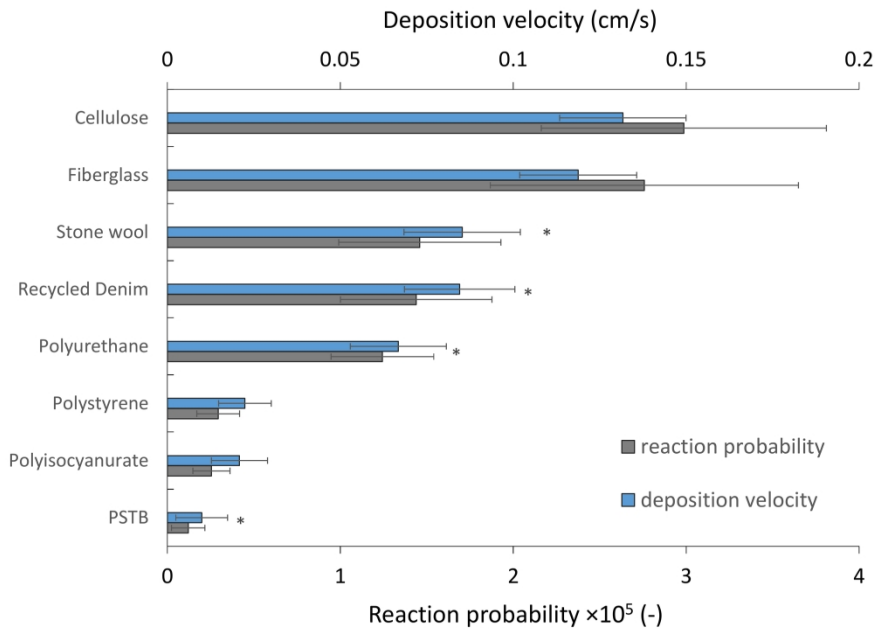


Figure 4. Summary of ozone deposition velocities and reaction probabilities calculated for each of the eight test materials. PSTB = Polystyrene with thermal backing.

*Note that γ for these materials were calculated using v_t measured for another tested material with similar surface morphology. The assumed v_t results in an additional source of uncertainty in the calculation of γ for these materials, described in greater detail in the supporting information in Table S4.

193x140mm (300 x 300 DPI)

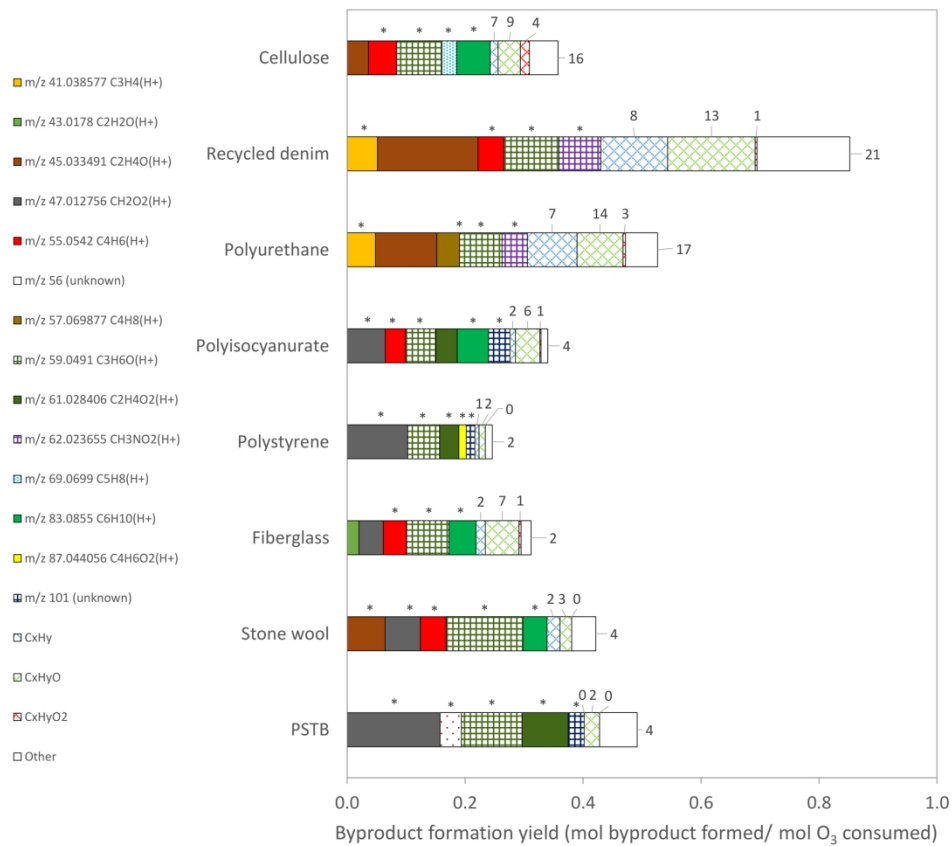
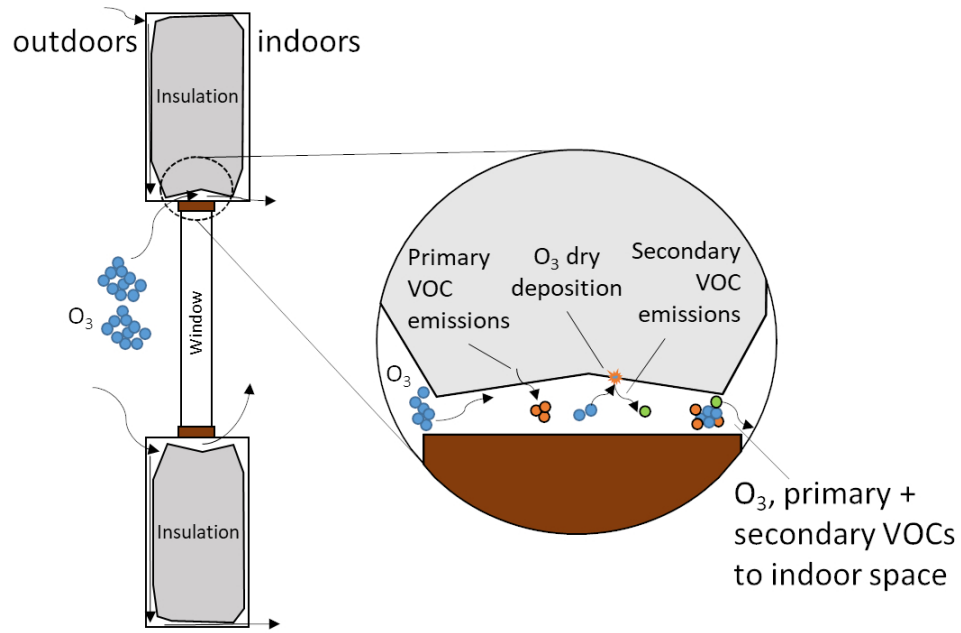


Figure 5. Summary of byproduct formation yields for each tested material. Note that the data labels on the C_xH_y, C_xH_yO, C_xH_yO₂, and Other categories refer to the number of unique, statistically significantly elevated compounds identified. Asterisks indicate compounds that were elevated in the presence of ozone and unique from those compounds observed in the primary emissions tests for that material. PSTB = polystyrene with thermal backing.

182x162mm (300 x 300 DPI)

1
2
3
4
5
6
7
8
9
10
11
12
13
14
15
16
17
18
19
20
21
22
23
24
25
26
27
28
29
30
31
32
33
34
35
36
37
38
39
40
41
42
43
44
45
46
47
48
49
50
51
52
53
54
55
56
57
58
59
60



TOC STATEMENT:

Emissions and oxidation chemistry occurring on building insulation materials may impact indoor levels of VOCs and ozone.

93x59mm (300 x 300 DPI)